Korean J. Chem. Eng., **28**(3), 744-750 (2011)
DOI: 10.1007/s11814-011-0019-3

Direct conversion of cellulose into polyols or H_2 over Pt/Na(H)-ZSM-5

Su Jin You*, In Gu Baek*, Yong Tae Kim*, Kwang-Eun Jeong, Ho-Jeong Chae**, Tae-Wan Kim**, Chul-Ung Kim**, Soon-Yong Jeong**, Tae Jin Kim***, Young-Min Chung***, Seung-Hoon Oh***, and Eun Duck Park*,†**

*Division of Energy Systems Research and Division of Chemical Engineering and Materials Engineering, Ajou University, San 5 Woncheon-dong, Yeongtong-gu, Suwon 443-749, Korea
**Korea Research Institute of Chemical Technology, Sinseongno 19, Yuseong-gu, Daejeon 305-600, Korea
***SK Energy Institute of Technology, Wonchon-dong, Yuseong-gu, Daejeon 305-712, Korea
(*Received 17 December 2010 • accepted 21 January 2011*)

Abstract−The direct conversion of cellulose into polyols such as ethylene glycol and propylene glycol was examined over Pt catalysts supported on H-ZSM-5 with different SiO_2/Al_2O_3 molar ratios. The Pt dispersion, determined by CO chemisorption and transmission electron microscopy (TEM), as well as the surface acid concentration measured by the temperature-programmed desorption of ammonia (NH_3-TPD), increased with decreasing SiO_2/Al_2O_3 molar ratio for Pt/H-ZSM-5. The total yield of the polyols, i.e., sorbitol, manitol, ethylene glycol and propylene glycol, generally increased with increasing Pt dispersion in Pt/H-ZSM-5. The one-pot aqueous-phase reforming of cellulose into H_2 was also examined over the same catalysts. The Pt catalyst supported on H-ZSM-5 with a moderate SiO_2/Al_2O_3 molar ratio and a large external surface area showed the highest H_2 production rate. The Pt dispersion, surface acidity, external surface area and surface hydrophilicity appear to affect the catalytic activity for this reaction.

Key words: Cellulose, Propylene Glycol, Aqueous-phase Reforming, H_2, Pt/H-ZSM-5

INTRODUCTION

Biomass is a renewable energy resource that can be transformed into various value-added fine chemicals; consequently, its utilization has attracted much attention. Biomass consists of a mixture of strongly bonded natural polymers such as cellulose (40-50%), hemicelluloses (25-30%), lignin and non-carbohydrate. Among them, cellulose is a quite attractive starting material for chemicals and fuel because it is abundant in nature and inedible. Cellulose consists of β-D-glucopyranose monomers linked together by β-1,4-glycosidic bonds. In spite of the abundance of hydroxyl groups in the monomer, it is hard to dissolve cellulose in water because of its robust crystalline structure with intense intermolecular and intramolecular hydrogen bonds. Indeed, cellulose with high crystallinity is resistant to chemical transformations. To overcome this drawback, which inhibits its wide utilization, cellulose has been pretreated physically and (or) chemically to decrease its degree of polymerization [1,2]. Therefore, the direct transformation of crystalline cellulose into value-added chemicals without any pretreatment is plausible. Aqueous-phase reactions would be suitable for this purpose, because it is confirmed that hydrothermal conditions would induce the degradation of the crystalline cellulose into amorphous species [3,4].

Various chemicals can be synthesized from glucose derived from cellulose. Especially, oxygen-containing fine chemicals can be formed under mild conditions, which is contrary to the present commercial route (i.e., partial oxidation under severe conditions) employed to produce the same products from fossil sources. Since Fukuoka and Dhepe [5] reported the transformation of cellulose into polyols via the aqueous-phase reaction in the presence of H_2, the direct conversion of cellulose into hexitols (sorbitol and manitol) was examined over supported Pt catalysts [5], Ru/C [6], Ru/CNT [7], Ru/C with heteropoly acids (HPAs) [8] or mineral acids [8,9] and ionic liquid-stabilized Ru^0 with a binding agent [10]. The transformation of crystalline cellulose into ethylene glycol was also reported over Ni-W_2C/AC [11,12], WC_x supported on mesoporous carbon and CMK-3 [13], Ni-WC_x/SBA-15 [14] and Ni_2P supported on AC and SiO_2 [15].

Besides value-added chemicals, the direct formation of H_2 from biomass-derived compounds via aqueous-phase reforming has attracted much attention. Ethylene glycol [16], glycerol [17], sorbitol [18] and glucose [19] can be directly transformed into H_2 at moderate temperatures. Furthermore, the one-pot synthesis of H_2 from crystalline cellulose over Pt/C via aqueous-phase reforming was reported [20].

In our previous work, we confirmed that Pt/AC showed the highest yield for ethylene glycol and propylene glycol among various noble metal (Pt, Ru, Ir, Rh, and Pd) catalysts supported on activated carbon [21]. Therefore, we selected Pt as the metal component and examined the effect of the support on the catalytic performance for the direct conversion of cellulose into polyols or H_2. Herein, we used Na-ZSM-5 and H-ZSM-5 with different SiO_2/Al_2O_3 molar ratios as the support for supported Pt catalysts to examine the effect of the surface acidity and surface hydrophilicity on the catalytic activity.

EXPERIMENTAL

1. Catalyst Preparation

Various ZSM-5 zeolites - NH_4-ZSM-5 (SiO_2/Al_2O_3=23, Zeolyst,

†To whom correspondence should be addressed.
E-mail: edpark@ajou.ac.kr

Table 1. The physicochemical properties of Pt/Na(H)-ZSM-5

Catalyst	Pt content (wt%)[a]	BET surface area (m^2/g)	Micropore surface area (m^2/g)[b]	External surface area (m^2/g)[b]	Micropore volume (cm^3/g)[b]	CO uptake (μmol $CO/g_{cat.}$)	CO/Pt (%)	The average particle size of Pt[c] (nm)	Total amount of acid sites (mmol $NH_3/g_{cat.}$)
Pt/Na-ZSM-5(23)	0.95	312	241	71	0.13	n.d.[d]	n.d.[d]	15.0±8.1	8.7×10^{-1}
Pt/H-ZSM-5(23)	0.97	256	146	110	0.07	25.5	52	1.4±0.8	6.1×10^{-1}
Pt/H-ZSM-5(30)	0.89	354	176	179	0.09	7.6	17	4.1±1.8	4.8×10^{-1}
Pt/H-ZSM-5(150)	0.90	422	212	211	0.11	6.3	14	4.5±1.7	1.3×10^{-1}
Pt/H-ZSM-5(500)	0.94	401	170	231	0.08	3.3	7	5.4±2.5	1.0×10^{-2}
Pt/H-ZSM-5(1000)	0.97	266	95	171	0.05	1.4	3	6.1±1.9	n.d.[d]

[a]The bulk composition was analyzed by ICP-AES
[b]The data were obtained by the t-plot method
[c]The average particle size of Pt was determined based on the bright-field TEM images
[d]Not detected

CBV2314, S_{BET}=572 m^2/g), H-ZSM-5 (SiO_2/Al_2O_3=30, Zeolyst, CBV3014E, S_{BET}=364 m^2/g), H-ZSM-5 (SiO_2/Al_2O_3=150, Süd-Chemie, S_{BET}=462 m^2/g), H-ZSM-5 (SiO_2/Al_2O_3=500, Zeocat, S_{BET}= 393 m^2/g), H-ZSM-5 (SiO_2/Al_2O_3=1,000, Zeocat, S_{BET}=292 m^2/g), and Na-ZSM-5 (SiO_2/Al_2O_3=23, Zeolyst, CBV2310, S_{BET}=449 m^2/g) - were purchased and utilized as a support after calcinations in air at 873 K. Therefore, NH_4-ZSM-5 was transformed into H-ZSM-5. To differentiate the supports, their SiO_2/Al_2O_3 molar ratios are presented in parentheses.

Pt/Na(H)-ZSM-5 catalysts were prepared by an incipient wetness impregnation method from the support and an aqueous solution of $Pt(NH_3)_4(NO_3)_2$ (Aldrich). The content of Pt was intended to be 1 wt%. If not expressed explicitly, all of the catalysts were calcined in air at 773 K and reduced in a hydrogen stream at 673 K for 1 h before the reaction.

2. Catalyst Characterization

The Pt content for all of the prepared catalysts was analyzed by inductively coupled plasma-atomic emission spectroscopy (ICP-AES, JY-70Plus, Jobin-Yvon) and listed in Table 1.

The BET surface area was calculated based on the N_2 adsorption data obtained using an Autosorb-1 apparatus (Quantachrome) at liquid N_2 temperature. Before the measurement, the sample was degassed in a vacuum for 6 h at 473 K. The micropore surface area, micropore volume, and external surface area for each catalyst were calculated by the t-plot method [22]. These data are presented in Table 1.

CO chemisorption was carried in an AutoChem 2,910 unit (Micromeritics) equipped with a thermal conductivity detector (TCD) to measure the CO consumption. Quartz U-tube reactors were generally loaded with the sample, and the catalysts were pretreated by reduction in H_2 at 673 K for 1 h and then cooled to room temperature. The CO chemisorption was carried out at 300 K in a He stream with a flow rate of 30 ml/min through the pulsed-chemisorption technique, in which 500 μl pulses of CO were utilized, after any residual hydrogen in the line was removed by flowing He at 300 K for 1 h.

The temperature-programmed desorption of ammonia (NH_3-TPD) was conducted in an AutoChem 2,910 unit (Micromeritics) equipped with a TCD to measure the NH_3 desorption and an on-line mass spectrometer (QMS 200, Pfeiffer Vacuum) to detect any organic or inorganic species in the effluent stream during the NH_3-TPD experiment. Quartz U-tube reactors were generally loaded with 0.10 g of the sample, and the catalysts were pretreated in He at 873 K 1 h and then cooled to 423 K. The charged sample was treated in 3 vol% NH_3/He at 423 K for 30 min and then the catalysts were flushed with He for 1 h. The NH_3-TPD was performed using 30 ml/min of He by heating the sample from 423 K to 873 K at a heating rate of 5 K/min while monitoring the TCD signals and mass signals.

Transmission electron microscopy (TEM) analysis was carried out by using a JEM-2100 F (JEOL) operated at 200 kV to determine the particle size of Pt metal. The samples were ground to fine particles in a mortar and then dispersed ultrasonically in methanol. The sample was deposited on a Cu grid covered by a holey carbon film.

3. Catalytic Performance Tests

The relative crystallinity of cellulose (Aldrich, microcrystalline) was determined to be 84% [21]. Its direct conversion into polyols was carried out in a batch reactor. 500 mg of cellulose and 50 mg of catalysts were mixed with 30 mL of deionized water and the resulting mixture was introduced into a stainless-steel autoclave with a volume of 85 mL. The reactor was filled with H_2 and the pressure was fixed at 6 MPa at ambient temperature. The slurry was stirred at a rate of 700 rpm. When the temperature reached the set point, the reaction time was regared as zero. After the reaction, the autoclave was cooled to room temperature and the solid residues were separated from the liquid products by centrifugation. The liquid product was filtered with a 0.2 μm membrane filter and analyzed with a bio-liquid chromatograph (HPAEC-PAD) equipped with a electrochemical cell pulsed amperometric detector (Dionex).

The one-pot aqueous-phase reforming of cellulose into H_2 was performed in the batch reactor described above. 990 mg of cellulose and 100 mg of catalysts were mixed with 45 ml of deionized water and the resulting mixture was introduced into a stainless-steel autoclave. The reactor was filled with 1 vol% N_2 in He as an internal standard and the pressure was fixed at 1 MPa at ambient temperature. The slurry was stirred at a rate of 700 rpm. When the temperature reached the set point, the reaction time was regarded as zero. After the reaction, the autoclave was cooled to room temperature. The gas product was analyzed by a gas chromatograph (HP 6890, Carbosphere column) equipped with a TCD.

The solid product was washed several times using deionized water and dried overnight at 353 K in a vacuum to evaluate the cellulose conversion. The cellulose conversion and yield for the products were calculated based on the following formulae:

$$X_C\,(\%)=(M_{C0}-M_C)/M_{C0}\times 100 \quad (1)$$

$$Y_P\,(\%)=M_{Pi}/(M_{C0}\times y_C)\times 100 \quad (2)$$

where X_C is the cellulose conversion, M_{C0} is the weight of cellulose before the reaction, M_C is the weight of cellulose after the reaction, Y_P is the yield of the products, M_{Pi} is the weight of carbon in the produced polyols and y_C is the weight fraction of carbon in cellulose determined by CHN analysis [21].

RESULTS AND DISCUSSION

The size and shape of the Pt metals used for the Pt catalyst supported on Na-ZSM-5(23) and H-ZSM-5 with different SiO_2/Al_2O_3 molar ratios were observed by TEM analysis, as shown in Fig. 1. Based on these data, the average particle size of the Pt metals was determined and is listed in Table 1. The average Pt particle size increased with increasing SiO_2/Al_2O_3 molar ratio in H-ZSM-5 for Pt/H-ZSM-5. On the other hand, the largest Pt particles with a wide particle size distribution were observed for Pt/Na-ZSM-5(23). This implies that the cations in ZSM-5 affect the interaction between $Pt(NH_3)_4^{2+}$ in the aqueous phase and the surface anchoring sites on the zeolites.

CO chemisorption was also carried out for all of the Pt/Na(H)-ZSM-5 catalysts to determine the number of CO adsorption sites on Pt metal (Pt_s : CO=1 : 1) and the results are listed in Table 1. The amount of chemisorbed CO increased with decreasing SiO_2/Al_2O_3 molar ratio in Pt/H-ZSM-5. This implies that the Pt dispersion decreased with increasing SiO_2/Al_2O_3 molar ratio for Pt/H-ZSM-5, which is identical to the TEM results. In the case of Pt/Na-ZSM-5 (23), no detectable amount of chemisorbed CO was observed, which implies that the particle size of Pt is very large.

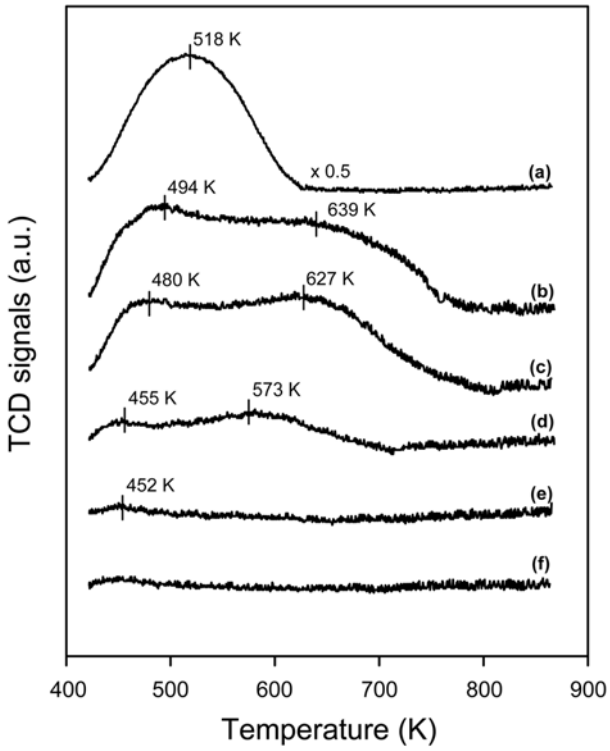

Fig. 2. Temperature-programmed desorption of ammonia (NH_3-TPD) patterns for Pt/Na(H)-ZSM-5 catalysts, viz. Pt/Na-ZSM-5(23) (a), Pt/H-ZSM-5(23) (b), Pt/H-ZSM-5(30) (c), Pt/H-ZSM-5(150) (d), Pt/H-ZSM-5(500) (e) and Pt/H-ZSM-5(1000) (f).

To determine the surface acidity of the Pt/Na(H)-ZSM-5 catalysts, NH_3-TPD was conducted and the TPD pattern for each catalyst was obtained, as shown in Fig. 2. A rather broad TPD peak with two distinguishable maxima in the low- and high-temperature regions was observed over Pt/H-ZSM-5 with SiO_2/Al_2O_3 molar ratios of 23,

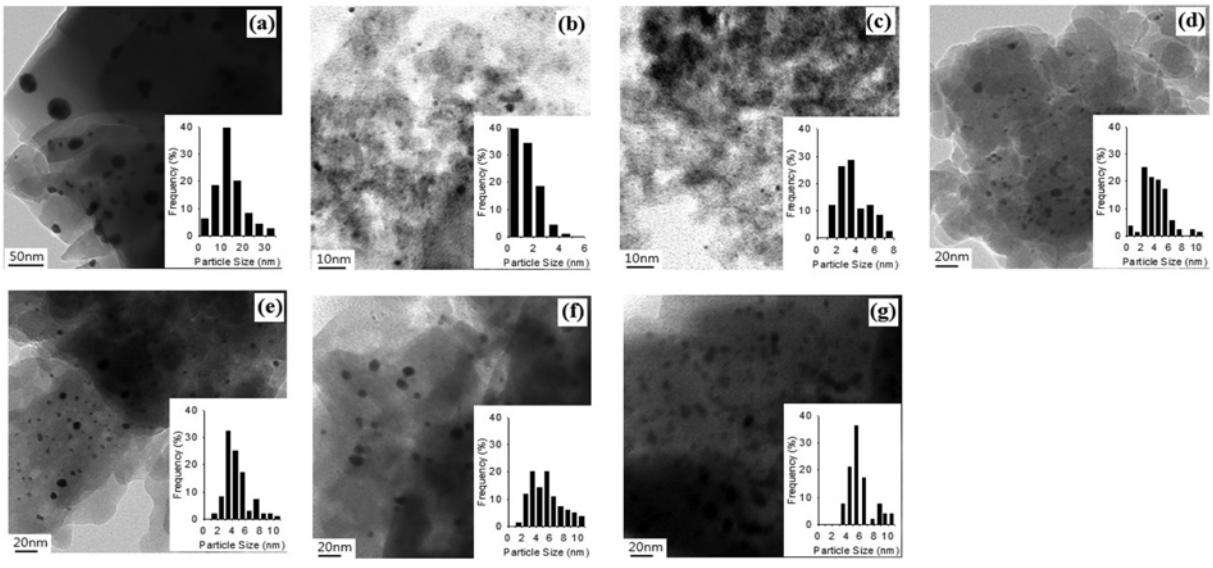

Fig. 1. The bright-field TEM image and the particle size distribution of Pt/Na-ZSM-5(23) (a), Pt/H-ZSM-5(23) (b), Pt/H-ZSM-5(23) reduced in H_2 at 873 K (c), Pt/H-ZSM-5(30) (d), Pt/H-ZSM-5(150) (e), Pt/H-ZSM-5(500) (f) and Pt/H-ZSM-5(1000) (g).

30 and 150. Only a weak TPD peak in the low-temperature region was found over Pt/H-ZSM-5 with SiO_2/Al_2O_3 molar ratios of 500 and 1,000. For Pt/Na-ZSM-5(23), only one distinguishable TPD peak can be observed in the low-temperature region. Based on the TPD data, the amount of surface acid sites was determined. Table 1 shows that the total amount of acid sites decreased with increasing SiO_2/Al_2O_3 molar ratio for Pt/H-ZSM-5. The largest total amount of acid sites was obtained over Pt/Na-ZSM-5(23). By comparing these data with those for the support itself [23], it was found that the total amount of acid sites was decreased slightly by the introduction of Pt. This implies that most of the surface acid sites were maintained, even in Pt/Na(H)-ZSM-5, and that Pt is mainly adsorbed on the acid sites on ZSM-5. Each Pt atom interacts with a Brønsted proton and with a nearby bridging framework oxygen in H-ZSM-5, resulting in the change in the electron density of the Pt atoms [24]. In our previous work [23], it was confirmed that Brønsted acid sites and Lewis acid sites were dominant for H-ZSM-5 and Na-ZSM-5(23), respectively. The difference in the types of surface acid sites might be responsible for the noticeable difference in the Pt dispersion between Pt/H-ZSM-5(23) and Pt/Na-ZSM-5(23). It was suggested that Pt atoms are not stable in H-ZSM-5 without the Brønsted acid sites, thus leading to their agglomeration to form larger particles [24].

The direct conversion of cellulose into polyols, i.e., sorbitol, manitol, ethylene glycol, and propylene glycol, was performed over the Pt/Na(H)-ZSM-5 catalysts, as listed in Table 2. Comparable conversions of cellulose were obtained in the absence of a catalyst with those in their presence. This can be explained by considering that water itself releases the reversible H^+ ions at high temperatures above 473 K and that these H^+ ions are capable of promoting the hydrolysis of cellulose, resulting in the formation of condensation products from the primary product and derivatives [6,25]. In the presence of a Pt catalyst, a further enhanced cellulose conversion was observed. The formation of ethylene glycol and propylene glycol was confirmed, even in the absence of a catalyst, but their yields were very low. Table 2 shows that the total yield of the polyols increased with decreasing SiO_2/Al_2O_3 molar ratio of H-ZSM-5 for the Pt/H-ZSM-5 catalysts. Pt/H-ZSM-5(23) showed the highest ethylene glycol yield among the tested Pt catalysts. Traces of hextols (sorbitol and manitol) were detected with very low yields. Interestingly, the main product was propylene glycol when Pt was anchored on H-ZSM-5. In the case of Pt/Na-ZSM-5(23), the total yield of the polyols was very low, even though it has the highest total amount of acid sites. Therefore, it may be said that the role of Pt metal in facilitating the formation of polyols is more important than that of the acid sites, because Pt/Na-ZSM-5(23) has a very low Pt dispersion. To prove this hypothesis, we prepared the Pt/H-ZSM-5(23) catalyst reduced at 873 K in H_2 to increase the Pt particle size, while maintaining its surface acidity, and applied it to this reaction. The average Pt particle size determined by TEM analysis increased to 3.7± 1.5 nm, as shown in Fig. 1 and the Pt dispersion measured by CO chemisorption decreased to 10%. The yield of propylene glycol decreased significantly over this catalyst. Therefore, it can be concluded

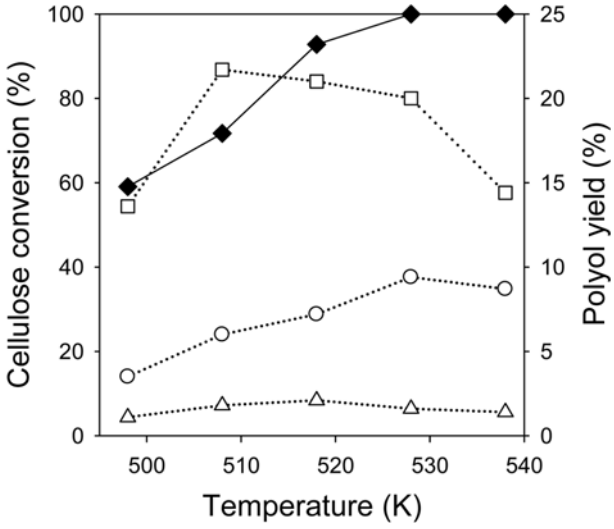

Fig. 3. Variations of the cellulose conversion and the yields of various polyols at different reaction temperature over Pt/H-ZSM-5(23). Left-hand axis: conversion of cellulose (◆); right-hand axis: yield of ethylene glycol (○), propylene glycol (□), and hexitols (△). Reaction conditions: the weight of cellulose=0.5 g, the weight of water=30 g, the weight of catalyst=50 mg; reaction time=2 h, H_2 pressure=6 MPa.

Table 2. The conversion of cellulose and product yields of various polyols for the direct conversion of cellulose into polyols over Pt/Na(H)-ZSM-5[a]

Catalysts	Conversion (%)	Yield (%)			
		Sorbitol	Manitol	Ethylene glycol	Propylene glycol
-	83	0.0	0.0	0.9	1.9
Pt/Na-ZSM-5(23)	98	0.8	0.0	2.0	0.9
Pt/H-ZSM-5(23)	93	1.3	0.8	7.2	21.0
Pt/H-ZSM-5(23)[b]	93	1.1	0.3	6.2	11.9
Pt/H-ZSM-5(30)	91	0.7	0.6	6.8	15.7
Pt/H-ZSM-5(150)	96	0.6	0.6	6.8	10.0
Pt/H-ZSM-5(500)	96	0.9	0.6	3.9	3.3
Pt/H-ZSM-5(1000)	91	0.2	0.0	1.5	1.0

[a]Reaction conditions: the weight of cellulose=50 mg, the volume of water=30 mL, the weight of catalyst=50 mg; reaction temperature=518 K, reaction time=2 h, initial H_2 pressure=6 MPa

[b]After reduction in H_2 at 873 K

that the Pt dispersion is an important factor for the direct conversion of cellulose into polyols.

To optimize the reaction conditions, the effect of the reaction temperature on the conversion of cellulose into polyols was examined over Pt/H-ZSM-5(23), as shown in Fig. 3. The cellulose conversion increased with increasing reaction temperature, and 100% conversion was achieved at temperatures higher than 528 K under the given conditions. The propylene glycol yield increased with increasing reaction temperatures, reaching a maximum of 22% at 508 K, and then decreased with further increasing reaction temperature. The ethylene glycol yield also increased with increasing reaction temperature, reaching a maximum of 9% at 528 K, and then slightly decreased with further increasing reaction temperature. The hexitol yield remained in the range of 1-2% at all reaction temperatures employed herein. These results imply that ethylene glycol and propylene glycol are reaction intermediates.

The effect of the reaction time on the conversion of cellulose into polyols was also examined over Pt/H-ZSM-5(23), as shown in Fig. 4. The cellulose conversion increased with increasing reaction time and 100% conversion was achieved at 6 h. The propylene glycol yield increased with increasing reaction time, reaching a maximum of 22% at 2 h, and then decreased with further increasing reaction time. The ethylene glycol yield also increased with increasing reaction time, reaching a maximum of 7% at 2 h, and then slightly decreased with further increasing reaction time. The yield of hexitols also increased with increasing reaction time, reaching a maximum of 2% at 2 h, and slightly decreased with further increasing reaction time. These results imply that the formation of ethylene glycol and propylene glycol are parallel rather than consecutive reactions.

The direct conversion of cellulose into H_2 was performed over the Pt/Na(H)-ZSM-5 catalysts, as listed in Table 3. The cellulose conversion increased with increasing SiO_2/Al_2O_3 molar ratio in the range from 23 to 150 for Pt/H-ZSM-5, showed the maximum values over Pt/H-ZSM-5(150), and then decreased with further increasing SiO_2/Al_2O_3 molar ratio for Pt/H-ZSM-5. A similar volcano plot can be made for the H_2 formation rate vs. SiO_2/Al_2O_3 molar ratio for Pt/H-ZSM-5, but no detectable amount of hydrogen was found over Pt/H-ZSM-5(500) and Pt/H-ZSM-5(1000), which have poor Pt dispersions and small amounts of weak surface acid sites. The formation of H_2 was not observed over Pt/Na-ZSM-5(23), which has the largest amount of weak Lewis acid sites but a very low Pt dispersion. Comparable cellulose conversions were obtained in the absence of any catalyst with those in the presence of the supported Pt catalysts. H_2 was also evolved in the absence of any catalyst although its formation rate was very low. These results imply that a bifunctional catalyst with a high Pt dispersion and strong acid sites is required to facilitate the direct formation of H_2 from cellulose. From this viewpoint, it might be thought that Pt/H-ZSM-5(23) should show the highest H_2 formation rate, but in reality Pt/H-ZSM-5(150) with a moderate Pt dispersion and amount of surface acid sites exhibited the best activity for this reaction. These results demonstrate that there is another important factor controlling this reaction. There have been some reports that zeolites with a moderate SiO_2/Al_2O_3 molar ratio show the highest catalytic activity. Onda et al. reported that hydrophobic zeolites, such as H-β and H-ZSM-5 with high SiO_2/Al_2O_3 ratios of 150 and 90, respectively, which prefer organic compounds to water, showed higher glucose yields than those of zeolites with a relative low SiO_2/Al_2O_3 ratio via the hydrolysis of cellulose [26]. Similar results were also observed for the production of glucose via the hydrolysis of maltose [27]. This allows us to speculate that the formation of glucose is a key intermediate step in the direct conversion of cellulose into H_2. Undoubtedly, in the case of H-ZSM-5, the amount of adsorbed H_2O and its binding strength decreases with increasing SiO_2/Al_2O_3 molar ratio [23]. The strong adsorption of H_2O was confirmed for Pt/Na-ZSM-5(23) [23]. Therefore, the surface hydrophilicity may be another factor controlling the catalytic activity for this reaction. It is also worth mentioning that the external surface area increased with increasing SiO_2/Al_2O_3 molar ratio in the case of H-ZSM-5 with SiO_2/Al_2O_3 molar ratios in the range from 23 to 500, as shown in Table 1. The external sur-

Table 3. The conversion of cellulose and the formation rate of H_2, CO, CH_4, and CO_2 for the direct conversion of cellulose over Pt/Na(H)-ZSM-5[a]

Catalysts	Conversion (%)	Formation rate ($\mu mol \cdot g_{cat.}^{-1} min^{-1}$)			
		H_2	CO	CH_4	CO_2
-	65	5.4	15.4	0.1	106.5
Pt/Na-ZSM-5(23)	70	0.0	13.7	0.2	124.2
Pt/H-ZSM-5(23)	72	30.4	0.9	4.6	205.9
Pt/H-ZSM-5(30)	73	39.7	1.4	5.2	214.0
Pt/H-ZSM-5(150)	77	67.4	0.4	9.8	316.6
Pt/H-ZSM-5(500)	67	0.0	9.5	0.2	106.7
Pt/H-ZSM-5(1000)	68	0.0	9.9	0.2	115.0

[a]Reaction conditions: the weight of cellulose=990 mg, the volume of water=45 mL, the weight of catalyst=100 mg; reaction temperature=518 K, reaction time=1 h, initial 1 vol%N_2/He pressure=1 MPa

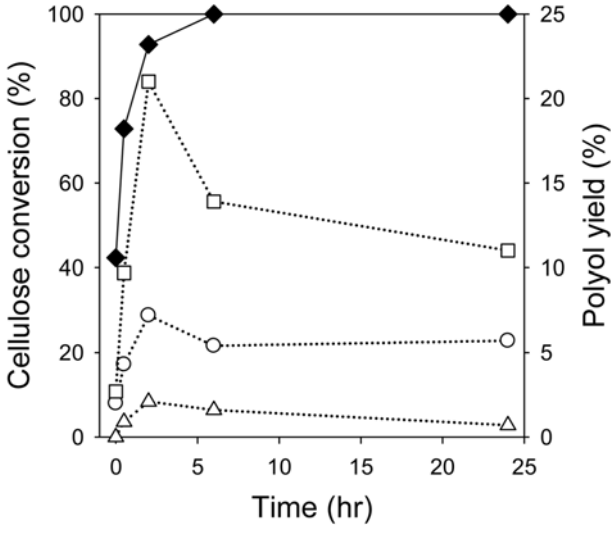

Fig. 4. Variations of the cellulose conversion and the yield of various polyols with reaction time over Pt/H-ZSM-5(23). Left-hand axis: conversion of cellulose (◆); right-hand axis: yield of ethylene glycol (○), propylene glycol (□), and hexitols (△). Reaction conditions: the weight of cellulose=0.5 g, the weight of water=30 g, the weight of catalyst=50 mg; reaction temperature=518 K, H_2 pressure=6 MPa.

face area is important when a bulky reactant, which is too large to penetrate into the micro channels in the zeolites, is involved. The larger the external surface area is, the more chance the bulky molecules have to interact with the active sites on the catalyst surface. The negligible H_2 formation rate observed over Pt/H-ZSM-5(500) with the largest external surface area can be explained by the fact it has a very low Pt dispersion and very small amounts of weak suface acid sites.

As shown in Table 3, a relatively large formation rate for CO was observed over the supported Pt catalysts with low Pt dispersions. Indeed, the largest CO formation rate was found in the absence of a catalyst. This can be ascribed to the fact that the rate of the water-gas shift reaction (WGS) is proportional to the Pt dispersion. The CH_4 formation rate is in line with the H_2 formation rate. There are various byproducts in the liquid phase, such as hydrolysis products, decomposed products (lactic acid, acetic acid and butyric acid) and furfural resins (5-HMF, furfuryl alcohol, 2-furaldehyde and acetyl furan) [28]. Dumesic et al. reported that the presence of Pt metal leads to the production of H_2 with high selectivity, whereas more acidic supports promote acid-catalyzed dehydration reactions and consecutive reactions during the aqueous-phase reforming of polyols [29].

Cellulose can be decomposed via two pathways: the hydrolysis reaction and retro-aldol condensation [30]. Under aqueous-phase reforming conditions (high water density), the hydrolysis of cellulose into glucose occurs predominantly. Further reforming reactions through the cleavage of the C-C bonds can proceed from the glucose and sorbitol formed by the hydrogenation of glucose [19,31]. Undesired alkanes can be formed by the cleavage of the C-O bonds and homogeneous side reactions can occur under these reaction conditions. The relatively low H_2/CO_2 ratio obtained in this work may be due to the consumption of H_2 in other side reactions, such as hydrogenation and hydrogenolysis reactions.

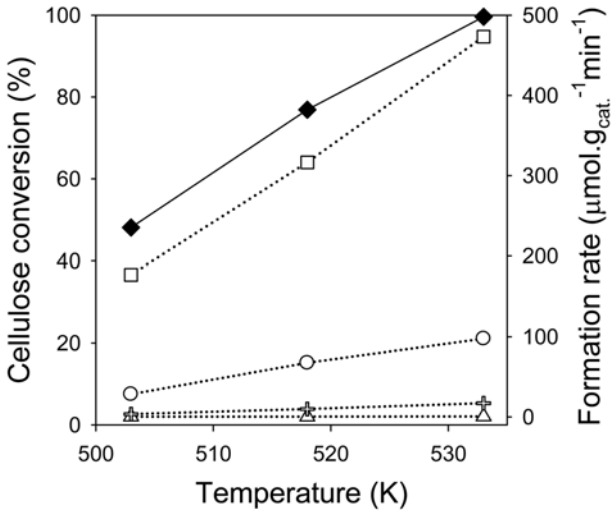

Fig. 5. Variations of the cellulose conversion and the formation rate of various gaseous products at different reaction temperature over Pt/H-ZSM-5(150). Left-hand axis: conversion of cellulose (◆); right-hand axis: formation rates of H_2 (○), CO_2 (□), CO (△) and CH_4 (+). Reaction conditions: the weight of cellulose=0.99 g, the weight of water=45 g, the weight of catalyst=0.10 g; reaction time=1 h, 1 vol% N_2/He pressure=1 MPa.

The effect of the reaction temperature on the direct conversion of cellulose into H_2 was examined over Pt/H-ZSM-5(150), as shown in Fig. 5. The cellulose conversion increased with increasing reaction temperature and 100% conversion was achieved above 533 K. The production rates for H_2, CO, CO_2 and CH_4 gradually increased with increasing reaction temperature. The H_2 formation rate at 533 K in this work is similar to the data obtained over Pt/C [20].

CONCLUSION

For the Pt/H-ZSM-5 catalysts prepared by the incipient wetness method, the Pt dispersion decreased with increasing SiO_2/Al_2O_3 molar ratio in H-ZSM-5. For Pt/Na-ZSM-5, a much lower Pt dispersion was observed compared with the case of Pt/H-ZSM-5. The total amount of acid sites decreased with increasing SiO_2/Al_2O_3 molar ratio for Pt/H-ZSM-5. For the direct conversion of cellulose into polyols in the presence of H_2, the total yield of the polyols increased with decreasing SiO_2/Al_2O_3 molar ratio in H-ZSM-5 for the Pt/H-ZSM-5 catalysts. It was confirmed that the Pt dispersion was an important factor in this reaction. On the other hand, Pt/H-ZSM-5 with a SiO_2/Al_2O_3 molar ratio of 150 showed the highest cellulose conversion, as well as the highest H_2 formation rate among the Pt/H-ZSM-5 catalysts with SiO_2/Al_2O_3 molar ratios in the range from 23 to 1,000 for the one-pot synthesis of H_2 from cellulose in the absence of H_2. For this reaction, it can be said that the Pt dispersion, surface acidity, external surface area, and surface hydrophilicity affect the catalytic activity, due to the complex reaction network.

ACKNOWLEDGEMENTS

This work was financially supported by a grant from the Industrial Source Technology Development Programs (10033099) of the Ministry of Knowledge Economy (MKE) of Korea.

REFERENCES

1. G. W. Huber, S. Iborra and A. Corma, *Chem. Rev.*, **106**, 4044 (2006).
2. P. L. Dhepe and A. Fukuoka, *ChemSusChem*, **1**, 969 (2008).
3. M. Sasaki, Z. Fang, Y. Fukushima, T. Adschiri and K. Arai, *Ind. Eng. Chem. Res.*, **39**, 2883 (2000).
4. S. Deguchi, K. Tsujii and K. Horikoshi, *Green. Chem.*, **10**, 191 (2008).
5. A. Fukuoka and P. L. Dhepe, *Angew. Chem. Int. Ed.*, **45**, 5161 (2006).
6. C. Luo, S. Wang and H. Liu, *Angew. Chem. Int. Ed.*, **46**, 7636 (2007).
7. W. Deng, X. Tan, W. Fang, Q. Zhang and Y. Wang, *Catal. Lett.*, **133**, 167 (2009).
8. J. Geboers, S. Van de Vyver, K. Carpentier, K. de Blochouse, P. Jacobs and B. Sels, *Chem. Commun.*, **46**, 3577 (2010).
9. R. Palkovits, K. Tajvidi, J. Procelewska, R. Rinaldi and A. Ruppert, *Green Chem.*, **12**, 972 (2010).
10. Y. Zhu, Z. N. Kong, L. P. Stubbs, H. Lin, S. Shen, E. V. Anslyn and J. A. Maguire, *ChemSusChem*, **3**, 67 (2010).
11. N. Ji, T. Zhang, M. Zheng, A. Wang, H. Wang, X. Wang and J. G. Chen, *Angew. Chem. Int. Ed.*, **47**, 8510 (2008).
12. N. Ji, T. Zhang, M. Zheng, A. Wang, H. Wang, X. Wang, Y. Shu,

A. L. Stottlemyer and J. G. Chen, *Catal. Today*, **147**, 77 (2009).
13. Y. Zhang, A. Wang and T. Zhang, *Chem. Commun.*, **46**, 862 (2010).
14. M. Y. Zheng, A. Q. Wang, N. Ji, J. F. Pang, X. D. Wang and T. Zhang, *ChemSusChem*, **3**, 63 (2010).
15. L. N. Ding, A. Q. Wang, M. Y. Zheng and T. Zhang, *ChemSusChem*, **3**, 818 (2010).
16. R. R. Davda, J. W. Shabaker, G. W. Huber, R. D. Cortright and J. A. Dumesic, *Appl. Catal. B: Environ.*, **43**, 13 (2003).
17. R. R. Soares, D. A. Simonetti and J. A. Dumesic, *Angew. Chem. Int. Ed.*, **45**, 3982 (2006).
18. G. W. Huber, R. D. Cortright and J. A. Dumesic, *Angew. Chem. Int. Ed.*, **43**, 1549 (2004).
19. R. R. Davda and J. A. Dumesic, *Chem. Commun.*, **10**, 36 (2004).
20. G. Wen, Y. Xu, Z. Xu and Z. Tian, *Catal. Commun.*, **11**, 522 (2010).
21. S. J. You, S. B. Kim, Y. T. Kim and E. D. Park, *Clean Technol.*, **16**, 19 (2010).
22. B. C. Lippens, B. G. Linsen and J. H. de Boer, *J. Catal.*, **3**, 32 (1964).
23. Y. T. Kim, K. D. Jung and E. D. Park, *Micropor. Mesopor. Mater.*, **131**, 28 (2010).
24. P. Treesukol, K. Srisuk, J. Limtrakul and T. N. Truong, *J. Phys. Chem. B*, **109**, 11940 (2005).
25. M. Sasaki, T. Adschiri and K. Arai, *AIChE J.*, **50**, 192 (2004).
26. A. Onda, T. Ochi and K. Yanagisawa, *Green Chem.*, **10**, 1033 (2008).
27. A. Abbadi, K. F. Gotlieb and H. van Bekkum, *Starch*, **50**, 23 (1998).
28. M. Sasaki, Z. Fang, Y. Fukushima, T. Adschiri and K. Arai, *Ind. Eng. Chem. Res.*, **39**, 2883 (2000).
29. R. R. Davda, J. W. Shabaker, G. W. Huber, R. D. Cortright and J. A. Dumesic, *Appl. Catal. B: Environ.*, **56**, 171 (2005).
30. Y. Matsumura, M. Sasaki, K. Okuda, S. Takami, S. Ohara, M. Umetsu and T. Adschiri, *Combust. Sci. Technol.*, **178**, 509 (2006).
31. R. D. Cortright, R. R. Davda and J. A. Dumesic, *Nature*, **418**, 964 (2002).